17

Base Isolation

Yeong-Bin Yang
and Kuo-Chun Chang
Department of Civil Engineering, National Taiwan University, Taipei Taiwan, R.O.C.

Jong-Dar Yau
Department of Architecture and Building Technology Tamkang University, Taipei Taiwan, R.O.C.

17.1 Introduction

Conventionally, seismic design of building structures is based on the concept of increasing the resistance capacity of the structures against earthquakes by employing, for example, the use of shear walls, braced frames, or moment-resistant frames. However, these traditional methods often result in high floor accelerations for stiff buildings, or large interstory drifts for flexible buildings. Because of this, the building contents and nonstructural components may suffer significant damage during a major earthquake, even if the structure itself remains basically intact. This is not tolerable for buildings whose contents are more costly and valuable than the buildings themselves. High-precision production factories are one example of buildings that contain extremely costly and sensitive equipment. Additionally, hospitals, police and fire stations, and telecommunication centers are examples of facilities that contain valuable equipment and should remain operational immediately after an earthquake.

In order to minimize interstory drifts, in addition to reducing floor accelerations, the concept of base isolation is increasingly being adopted. Base isolation (BI) has also been referred to as passive control, as the control of structural motions is not exercised through a logically driven external agency, but rather through a specially designed interface at the structural base or within the structure, which can reduce or filter out the forces transmitted from the ground. In contrast, the techniques of active or structural control, which are still under research and development for the seismic resistance of structures, require the installation of some logically controlled external agencies, such as actuators, to counteract the structural motions. One drawback with active control techniques is the relatively high cost of maintenance for the control system and actuators, which should remain functional at all times in order to respond to a major earthquake. There also exists a third category of techniques, called hybrid control, that make use of the best of both passive control and active control devices. In this chapter, there is no discussion of either active or hybrid control.

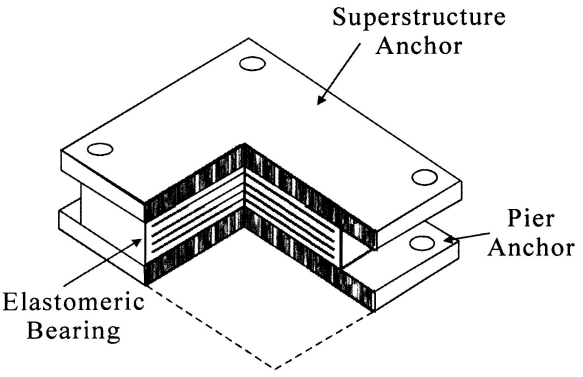

FIGURE 17.1 Elastomeric bearing.

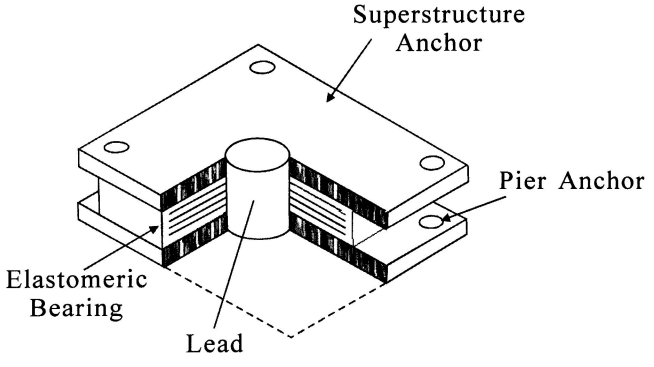

FIGURE 17.2 Laminated rubber bearing with lead core.

The effect of base isolation can be achieved through installation of certain devices between the building and the supporting foundation, so as to separate or *isolate* the motion of the building from that of the ground, making them basically uncoupled. The applicability of the concept of base isolation need not be restricted to the structure in its entirety. It can be applied as well to the isolation of sensitive equipment mounted inside a building from undesired floor vibrations through, for example, installation of an isolation system between the equipment base and the supporting floor. There are generally two basic approaches to base isolation, which have certain features in common.

One approach is to install some bearings of relatively low horizontal stiffness, but high vertical stiffness, between the structure and its foundation. With such devices, the natural period of the structure will be significantly lengthened and shifted away from the dominant high frequency range of the earthquakes. The elastomeric bearing shown in Figure 17.1 is typical of this category, which is composed of alternating layers of steel and hard rubber and, therefore, is also known as a laminated rubber bearing. This type of bearing is stiff enough to sustain vertical loads, yet is sufficiently flexible under lateral forces. The ability to deform horizontally enables the bearing to reduce significantly the shear forces induced by the earthquake. While the major function of elastomeric bearings is to reduce the transmission of shear forces to the superstructure through lengthening of the vibration period of the entire system, they should provide sufficient rigidity under the service load levels for wind and minor earthquakes. In reality, the reduction in seismic forces transmitted to the superstructure through installation of laminated rubber bearings is achieved at the expense of large relative displacements across the bearings. If substantial damping can be introduced into the bearings or the isolation system, then this large displacement problem can be alleviated. It is for this reason that the laminated rubber bearing with inclusion of a central lead plug has been devised, as shown in Figure 17.2. Other forms of supplemental dampers, such as hydraulic dampers, steel coils, and viscous dampers, also serve to increase the damping of the isolated structure.

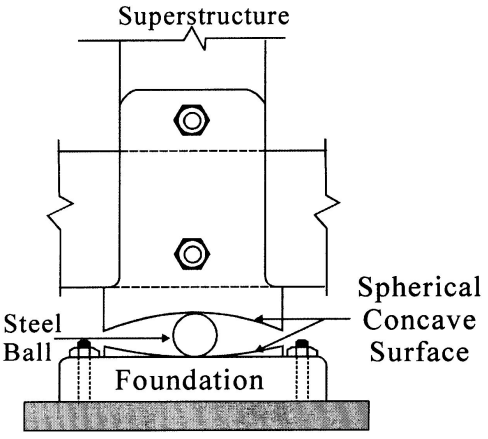

FIGURE 17.3 Friction pendulum system.

The other approach for increasing flexibility in a structure is to provide a *sliding* or *friction surface* between the foundation and the base of the structure. The shear force transmitted to the superstructure across the isolation interface is limited by the static friction force, which equals the product of the coefficient of friction and the weight of the superstructure. The coefficient of friction is usually kept as low as is practical. However, it must be sufficiently high to provide a friction force that can sustain strong winds and minor earthquakes without sliding. One particular problem with a sliding structure is the residual displacements that occur after major earthquakes. To remedy this problem, the sliding surface is often made concave so as to provide a recentering force. This is the idea behind the most popular frictional device, the so-called friction pendulum system (FPS), which utilizes a spherical concave surface, as shown in Figure 17.3. To guarantee that a sliding structure can return to its original position, other mechanisms, such as high-tension springs and elastomeric bearings, can be used as an auxiliary system to generate the restoring forces. Sliding isolation systems have been successfully used for nuclear power plants, emergency fire water tanks, large chemical storage tanks, and other important structures.

Numerous researchers have studied the dynamic behaviors of base-isolated structures under earthquakes using different devices for seismic isolation. Skinner et al. [1993] provided a comprehensive study on the application of isolation devices to practical structures. As for the application of rubber bearings to seismic design, Kelly [1993] gave a detailed procedure for the analysis of rubber isolation systems mounted on building structures. However, for base-isolated buildings located at near-fault sites, the design engineer is faced with very large design displacements for the isolators. To reduce these displacements, some researchers and design engineers suggested the addition of supplemental dampers alongside the isolators [Hall, 1999; Hall and Ryan, 2000]. It was argued by Kelly [1999] that increasing the damping in an isolation system may result in significant increase in the floor accelerations and interstory drifts of the isolated buildings. He went on to suggest some alternative strategies for overcoming this problem, such as the adoption of a gradual increasing curvature for the disk of the friction pendulum system, and the use of increased stiffness and increased damping for elastomeric isolators.

A review of the isolation devices that have been studied and used from 1900 to 1984 was conducted by Kelly [1986]. In general, most isolation systems are nonlinear in terms of the force–displacement relationships. For a wide range of problems encountered, however, a linear analysis of the base-isolated structure using simple models allows us to gain insight into the dynamics of these systems, while identifying the key parameters involved [Chopra, 1995]. With such an approach, the superstructure of the base-isolated structure is often assumed to be elastic and even treated as a single-degree-of-freedom (SDOF) system, the elastomeric bearing as a combination of elastic spring and viscous damper, and the sliding surfaces as flat surfaces obeying the law of static friction. It should be realized that in the final stage of design, the nonlinear properties of the base isolators or their effects should be taken into account.

Considering the geometric and material nonlinearities of elastomeric bearings with high damping rubber, Salomon et al. [1999] proposed a finite element model for analyzing base-isolated buildings with elastomeric isolators. Concerning the effect of torsional coupling on the seismic response of a base-isolated structure, an analytical study was carried out by Jangid and Kelly [2000]. Their results indicated that the effect of torsional coupling can significantly influence the response of the isolated structure but, when the torsional frequency is larger than the lateral frequency, the effect is reduced. Using the Rayleigh-Ritz procedure, Ryan and Chopra [2002] presented three approximate methods for analyzing the eccentricity effect of an asymmetric-plan base-isolated building subjected to ground motions. They concluded that the rigid structure method, which is often used for studying the dynamics of base-isolated systems, is not suitable for systems with zero isolation eccentricity, due to neglect of the structural flexibility and eccentricity.

As for sliding structures, the most fundamental theories have been laid out in the works by Westermo and Udwadia [1983] and Mostaghel et al. [1983]. The effect of higher modes of vibration on multi-degree-of-freedom (MDOF) structures was investigated by Yang et al. (1990), in which the concept of a fictitious spring was adopted to overcome the discontinuities encountered in analysis of the sliding and nonsliding phases of the system. Also, using the concept of fictitious springs, the dynamics of equipment mounted in a sliding structure was studied by Lu and Yang [1997]. For friction pendulum systems with spherical sliding surfaces, Tsai [1997] suggested that the local bending moment effects be considered for isolated structures to ensure their safety during earthquakes.

The book written by Naeim and Kelly [1999] dealt particularly with the procedural aspects of design for seismic isolated structures. In the chapter by Mayes and Naiem [2001], the most recent International Building Code [ICC, 2000] design provisions for seismic isolation were discussed in detail, along with the procedures of design for various isolators. The objective of this chapter is to provide a rather practical coverage of the design procedures for base isolators used in building structures.

17.2 Philosophy behind Seismic Isolation Systems

When a structure is subjected to a strong earthquake, the system energy of the structure can be conceptually expressed as:

$$KE + DE + SE = IE \tag{17.1}$$

where *KE* denotes the kinetic energy, *DE* the dissipated energy, which equals the sum of *VE* and *HE*, with *VE* denoting the viscous energy and *HE* the hysteretic energy; *SE* is the strain energy and *IE* the seismic input energy.

In Equation 17.1, *KE* and *SE* are the portion of the energy of the structure that is recoverable, whereas *VE* and *HE* are the portion that is dissipative. For a fixed-base building structure, when *IE* is not so large, the energy input to the structure will be dissipated in the form of *VE*. When a strong earthquake occurs, if all the input energy cannot be dissipated by the viscous damping of the structure, then the residual energy will be dissipated in the form of *HE*. If the structure has been designed to have sufficient ductility, then it may undergo plastic deformations in certain joints, members or specially added components, but the phenomenon of collapse must be avoided. This is the ductility concept of design for the traditional fixed-base structures.

The dynamic characteristics of a base-isolated building can be modeled as a single-story building with a linear isolator, as shown in Figure 17.4. Let us assume that the mass and rigidity of the base-isolated building are much greater than those of the isolators. By treating the isolated part of the building as a rigid mass, the base-isolated building can be simulated as an SDOF system, for which the equation of motion is:

$$M\ddot{u} + C\dot{u} + Ku = -M\ddot{u}_g \tag{17.2}$$

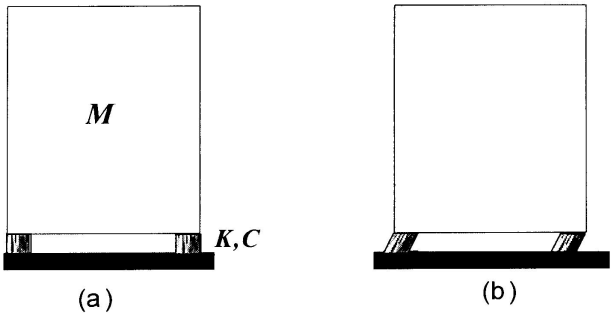

FIGURE 17.4 Isolated structure: (a) initial position, (b) deformed position.

where $\ddot{u}_g$ denotes the ground acceleration, u the displacement of the structure, M the mass of the structure, C the damping, and K the stiffness of the isolator.

By Duhamel's integral, the response $u(t)$ of the base-isolated system can be given by:

$$u(t) = \frac{1}{\omega_d}\int_0^t -\ddot{u}_g(\tau)e^{-\xi\omega(t-\tau)}\sin\omega_d(t-\tau)d\tau \tag{17.3}$$

where the natural frequency ω, damped natural frequency ω_d, and damping ratio ξ are defined as follows:

$$\omega = \sqrt{\frac{K}{M}}, \quad \omega_d = \omega\sqrt{1-\xi^2}, \quad \xi = \frac{C}{2M\omega} \tag{17.4}$$

Correspondingly, the natural period of vibration, T, and the natural period of damped vibration, T_d, are:

$$T = \frac{2\pi}{\omega} = 2\pi\sqrt{\frac{M}{K}}, \qquad T_d = \frac{2\pi}{\omega_d} = \frac{T}{\sqrt{1-\xi^2}} \tag{17.5}$$

For a given ground motion $\ddot{u}_g$, the deformation and acceleration responses, u and $\ddot{u}$, of an SDOF structure depend only on the natural period of vibration T and damping ratio ξ of the structure. Thus, for a specific earthquake, by first selecting a damping ratio ξ, one can compute the peak deformation u for a structure with a period of vibration T, i.e., with given values of M, C, K, using Equation 17.3. Repeating such a procedure for a wide range of period T, while keeping the damping ratio ξ constant, provides one curve similar to those shown in Figure 17.5. By varying the damping ratio ξ, one can construct the *deformation response spectra* for all SDOF structures under a given earthquake, as shown schematically in Figure 17.5.

The pseudo-acceleration response $A(t)$ of a system can be computed from the deformation response $u(t)$ of the system by:

$$A(t) = \omega^2 u(t) = \left(\frac{2\pi}{T}\right)^2 u(t) \tag{17.6}$$

In seismic engineering, the pseudo-acceleration response $A(t)$ is an important quantity, since it can be multiplied by the mass M to yield the *equivalent static force* or *base shear* of the structure considered. The *pseudo-acceleration response spectra*, as shown schematically in Figure 17.6, represent plots of the peak value of $A(t)$ with respect to the natural period of vibration T of the structure, which can be obtained

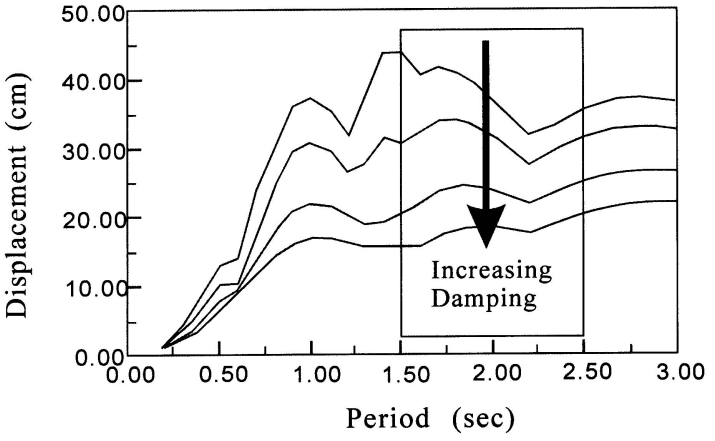

FIGURE 17.5 Schematic of deformation response spectra.

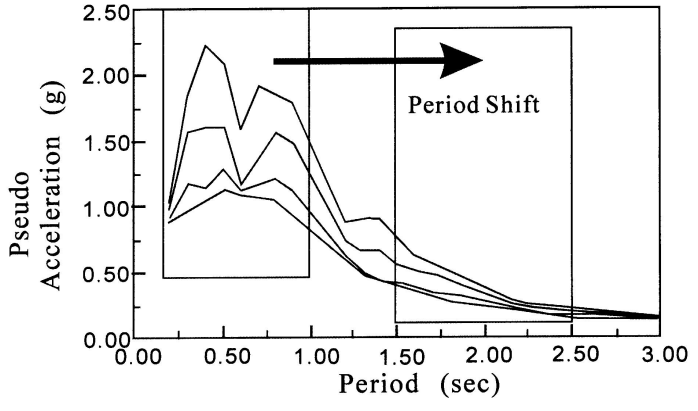

FIGURE 17.6 Schematic of pseudo-acceleration spectra.

as a by-product of the deformation response spectra shown in Figure 17.5 through use of the relation in Equation 17.6.

Two important features can be observed from the response spectra given in Figures 17.5 and 17.6. The first is the so-called *period shift* effect. As indicated by Figure 17.6, substantial reduction in the pseudo-acceleration or the base shear of a structure is possible, if the period of vibration of the structure is significantly lengthened, for example, through installation of base isolators. The level of reduction depends primarily on the nature of the ground motion and the period of the fixed-base structure. In general, the additional flexibility needed to lengthen the period of the structure will give rise to large relative displacements across the isolators, as indicated by Figure 17.5. The second is the so-called *energy dissipating* effect. If additional damping is introduced into the structure, then the deformation of the structure can be significantly reduced (see Figure 17.5). Also, it can be seen that a smaller base shear force will be induced on a structure should it have larger damping (see Figure 17.6), and that a structure responds less sensitively to variations in ground motion characteristics, as indicated by the smoother response curves for structures with higher damping levels in both figures.

As revealed by the aforementioned two seismic response spectra, the philosophy behind the installation of base isolators is to *lengthen the period of vibration of the protected structure, so as to reduce the base shear induced by the earthquake, while providing additional damping for reducing the relative displacements across the isolators themselves*. This is why most seismic design codes suggest the use of base isolation systems that have the dual function of period elongation and energy dissipation. Moreover, it

is required that the isolators be stiff enough under service load levels, e.g., under the wind loads or minor earthquakes, so as not to create frequent vibration annoyances to the occupants.

Two additional factors should be considered before base isolation is regarded as a feasible means for aseismic design [Mayes and Naeim, 2001]. First, most benefits of base isolation can be achieved only for stiff structures, i.e., with a fixed-base fundamental period of 1.0 sec or less. For these structures, the fundamental period can be elongated to the range of 1.5 to 2.5 sec through the installation of base isolators, resulting in the largest margin that can be achieved for period shifting. Clearly, base isolation is a technique most applicable to low-rise and medium-rise buildings, and less effective for high-rise buildings, as the natural period of vibration of a building generally increases with increasing height. It is not uncommon that the natural periods of high-rise buildings are so long that their design is governed in general by wind loads, rather than by earthquake loads. If there still exist concerns for improving the performance of high-rise buildings, then energy dissipation devices, including tuned-mass dampers, that do not depend on lengthening of the structural periods, should be considered.

The second factor to be considered is soil condition. When we mention earthquakes, we mean the ground motion $\ddot{u}_g$ used as the input to the base of the isolated system in Equation 17.2, based on which the response spectra in Figures 17.5 and 17.6 have been constructed. The form of the ground motion $\ddot{u}_g$, as it arrives at the base of a structure, will be filtered by the properties of the underlying soils through which the earthquake waves travel. For hard soils, the ground motion $\ddot{u}_g$ is composed mainly of high frequency components, while for soft soils, it is dominated by low frequency components. All these properties will be carried over to the response spectra constructed for the particular earthquake. At this point, it should be mentioned that the seismic response spectra shown schematically in Figures 17.5 and 17.6 are typical of earthquakes that have a predominance of high frequency (or low-period) ground motions, in the range of 0.1 to 1 sec. It is for this kind of earthquake, and the stiff soil conditions it implies, that the concept of base isolation is most applicable.

There exist cases where the ground motion $\ddot{u}_g$ is dominated by low frequency ground vibrations. One extreme example was the 1985 Mexico City earthquake, which contained a significant portion of long-period vibrations, in the range of 1.5 to 2.5 sec, as the city is located in a soft lake-bed. For this kind of soil condition, larger response will be expected for structures with a fundamental period in the range of 1.5 to 2.5 sec, which is exactly the desired range that is supposed to be achieved through installation of base isolators for structures. Thus, lengthening of the period of a stiff structure will not result in reduction, but rather amplification, of the base shear. Obviously, for structures located on soft soil strata, the application of base isolators is not helpful, but harmful. For the purpose of reducing the structural response, one can only have recourse to energy-dissipating devices, such as viscous dampers and hydraulic dampers.

17.3 Basic Requirements of Seismic Isolation Systems

A practical seismic isolation system should meet the following three requirements:

1. Sufficient horizontal flexibility to increase the structural period and spectral demands, except for very soft soil sites
2. Sufficient energy dissipation capacity to limit the displacements across the isolators to a practical level
3. Adequate rigidity to make the isolated building no different from a fixed-base building under general service loading

Most commonly used seismic isolating systems can satisfy all the above requirements. Certainly, if the seismic isolating system can be equipped with fail-safe devices for avoiding the total collapse of the isolated structure in cases where excessive displacements occur, then the system will most likely be satisfactory.

In the past two decades, the technology of seismic isolation has evolved along the lines of similar principles, resulting in the invention of one isolation device after the other [Johnson and Kienholz, 1982; Dynamic Isolation System, 1990; Bridgestone, 1990; Earthquake Protection Systems, 1993]. Most of the

seismic isolation devices available in the market satisfy the basic requirements identified above, while having their own characteristics. Commercially available seismic isolation systems can be classified according to their dynamic characteristics and how they are formed from individual devices.

The combination of elastomeric bearings and dampers represents a broad category of seismic isolators that have been used. The elastomers used by this kind of seismic isolators are usually made of natural rubber. Depending on how the elastomeric bearings and dampers are combined, this kind of seismic isolators can be further divided into two categories, as *single-combination* and *separate-combination*. In the single-combination, a single unit of isolator can provide the dual function of horizontal flexibility and energy dissipation. One typical example is the lead-rubber bearing (LRB), which combines the natural rubber bearing with a central lead core (Figure 17.2). In the separate-combination, the elastomeric bearings are supplemented by a number of dampers in separate units. The dampers used in this regard include:

- The yielding type dampers or hysteretic dampers that are made of steel plates, steel bars, steel rings, and the like
- The viscous dampers that are made of viscous materials, silicon fluid, etc. [Iwan and Gates, 1979; Iwan, 1980]

The high damping rubber bearing (HDR) is similar in shape to the elastomeric bearing shown in Figure 17.1, except that it is made of specially compounded rubber that exhibits effective damping between 0.1 and 0.2 of critical. Because the ingredients used by each design firm in producing the HDR are generally different, drastic differences in the dynamic properties of the HDRs produced by various firms can be observed. One common feature of these dampers is that they all share the desired feature of high damping capacity.

The most popular friction or sliding systems that apply low frictional interfaces to reduce the transmission of shear force to the isolated structure include the Electricite de France (EDF) system, resilient-friction base isolator (R-FBI), friction pendulum systems (FPSs) (see Figure 17.3), and Teflon and polished stainless steel formed sliding systems. As for the EDF system, the sliding surface is linked to neoprene bearings and the isolated structure has the potential of sliding downward due to inhomogeneous settlement of the isolation system. For the R-FBIs containing a rubber core in the center, blocking may occur and concentrate in certain Teflon layers. If a steel bar is inserted in the center of the R-FBI to drive all Teflon layers with the same level of sliding, then the problem of being unable to return the structure to its original position usually exists after a strong earthquake.

Compared with the elastomeric and LRB bearings, most friction systems have the advantage that they are not affected either by the natural frequency of the isolated structure or the frequency content of the earthquake. The coefficient of friction is the key parameter that determines whether or not sliding will occur with the system. However, most friction systems have the drawback that they are incapable of returning the structure to its original position. It is likely that permanent offset may exist between the sliding parts of the system after a major earthquake.

The problem of permanent offset or residual displacements can be overcome through use of the FPS shown in Figure 17.3, for which the sliding surface takes a spherical shape. For a spherical sliding surface, the radius of curvature R is constant, so that the bearing exhibits a linear restoring force, that is, under the constant gravity load W the stiffness is equal to W/R [Zayas et al., 1987]. The advantages of the FPS include the following: relatively small construction cost, small net-height required for installation, high vertical rigidity, well-proved durability against temperature and corrosion, and coincidence of mass center with shear center, which implies small torsional effects. For these reasons, the FPS is becoming one of the most popular friction systems used in seismic isolation.

Each of the seismic isolation systems mentioned above has specific dynamic properties and functions. Even for isolators of the same category, it is likely that variations in material properties may exist among the products offered by different manufacturers. Moreover, since most of the isolation systems reported in the literature are patented products (the same is also true with most newly invented products), not all of them are readily available for procurement and application. In preparing this chapter on base

isolation, we can only use those materials that are readily available to us. No intention is made to refer to any specific products. If any data have been included, they are considered mainly for the purpose of illustration. Although the general principles of design remain valid, it is the responsibility of the designers to verify that the cases presented in the following sections can really fit their situations.

17.4 Design Criteria for Isolation Devices

A complete design for base isolation should ensure that the isolators can support the maximum gravity service loads of the structure throughout its life, and the isolators can provide the dual function of period shift and energy dissipation to the isolated structure during earthquakes. In accordance with these design aims, the following design steps should be undertaken [Mayes and Naeim, 2001]:

1. Determine the minimum plan size required and locations of isolators under the maximum gravity loads
2. Compute the dimensions of the isolators that will result in the desired period shift for reducing the earthquake forces
3. Determine the damping ratio of the isolator such that the displacement of the structure can be controlled within the design limit under wind loads
4. Check the performance of the isolators under gravity, wind, thermal, earthquake, and other possible load conditions

To implement the design procedure for the seismic isolators, three different isolation systems, that is, the high damping rubber bearing, lead-core rubber bearing, and FPS, are considered in this chapter. The primary purpose herein is to illustrate the concepts involved in the preliminary sizing of isolators for a given project.

17.5 Design of High Damping Rubber Bearings

The rubber layers constituting the high damping rubber bearing (HDR) are usually made of materials that are highly nonlinear in terms of shear strains. Effective damping in the range of 0.10~0.20 of critical can easily be exhibited by the HDR, which is achieved through addition of special chemical compounds that can change the material properties of the rubber. As was stated previously, the stiffness and damping of the HDR are required to be large enough to resist wind and minor earthquakes. In practice, the stiffness and damping properties of the HDR remain quite stable under one or more design earthquakes. Thus, similar to what has been undertaken in most previous studies, the HDR is assumed to be linear elastic and isotropic in this chapter, for the purpose of preliminary design.

17.5.1 Design Flow Chart for HDR Bearings

The design flow chart for the high damping rubber bearings is shown in Figure 17.7. In the following, each of the parameters is defined at the place where it first appears, unless it is given a different meaning. The design procedure for the HDR is explained as follows:

1. Specify the soil condition for the isolated structure.
2. Select the design shear strain γ_{max} and effective damping ratio ξ_{eff} for the bearing, and the target design period T_D for the isolated structure. The former can be obtained from the material supplier.
3. Use code formulas, or static or dynamic analysis, to determine the effective horizontal stiffness K_{eff} and maximum horizontal (design) displacement D of the bearing.
4. Select the material properties, including Young's modulus E and shear modulus G, from the manufacturer's test report.
5. Calculate the total height of rubber, t_r, in the bearing according to the design displacement D and design shear strain γ_{max}:

$$t_r = \frac{D}{\gamma_{max}} \tag{17.7}$$

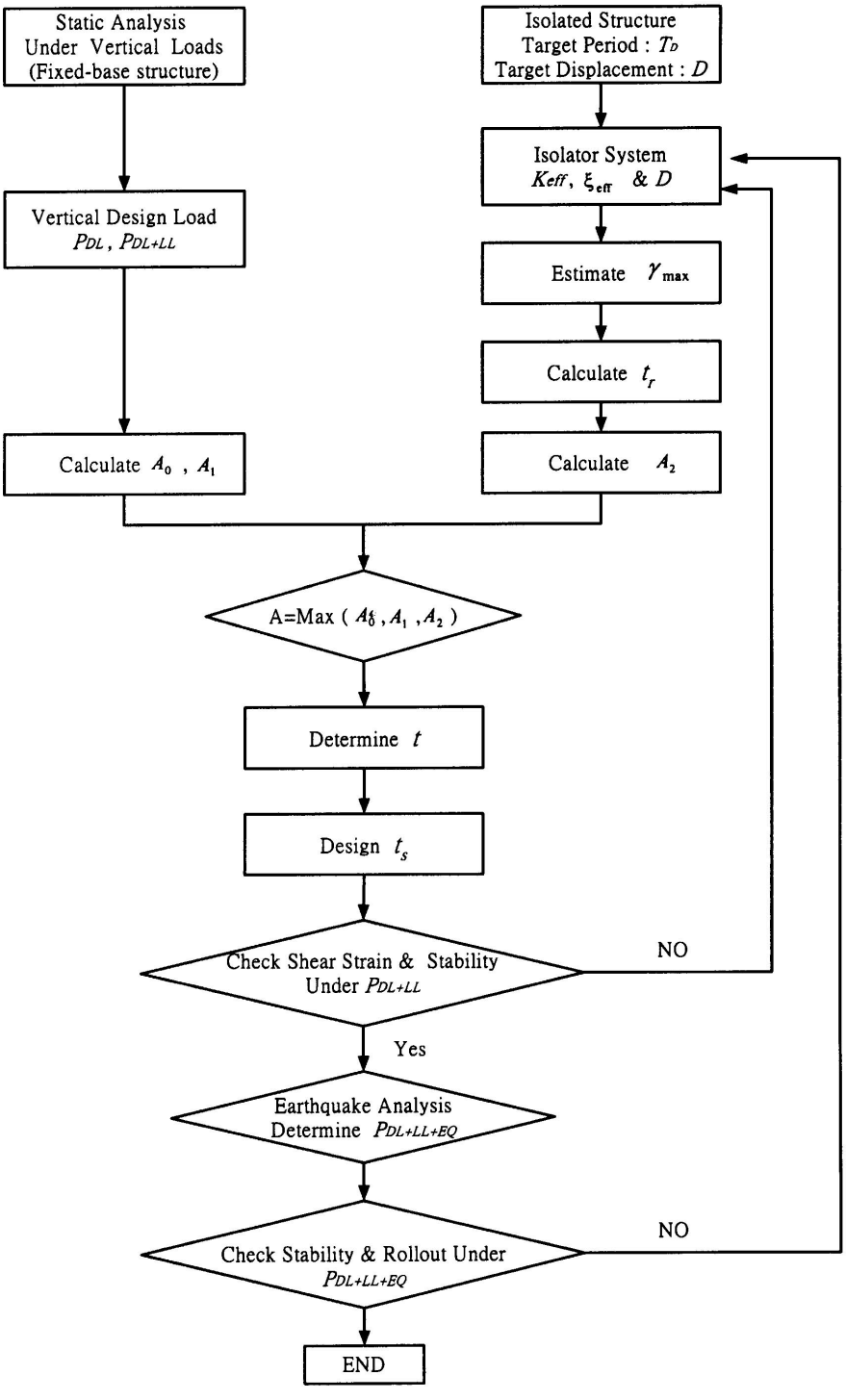

FIGURE 17.7 Design flow chart for HDR.

6. Calculate the effective area A and thickness t of individual rubber layers.
   a. Select the shape factor S under no rocking condition:

$$\frac{K_v}{K_h} = \frac{\dfrac{E_c \cdot A}{t_r}}{\dfrac{G \cdot A}{t_r}} = \frac{E_c}{G} = \frac{E \cdot \left(1 + 2\,kS^2\right)}{G} \geq 400 \quad \text{for} \quad S > 10 \tag{17.8}$$

where

K_v = vertical stiffness of the bearing
K_h = horizontal stiffness of the bearing
G = shear modulus, in the range of 0.4 to 1.0 MPa
E = Young's modulus, in the range of 1.5 to 5.0 MPa
E_c = compression modulus of the rubber-steel composite, $E_c = E(1 + 2kS^2)$
A = full cross-sectional area (loaded area) of the bearing
t_r = total height of rubber layers
k = modified factor, in the range of 1 to 0.5
S = shape factor = A/A_f [Kelly, 1993]
A_f = load-free area around the bearing (Figure 17.8)

In Equation 17.8, the stiffness ratio K_v/K_h is required to be greater than 400 for $S > 10$, since the P-δ effect has been ignored in computing the horizontal stiffness K_h. The material constants G, E, and k can be related to the rubber hardness, say, similar to those shown in Table 17.1 [Bridgestone, 1990]. If no published data are available, G and E should be determined by test.

   b. Determine the effective cross-sectional area A_0 of the bearing based on the allowable stress σ_c for the vertical load case P_{DL+LL}:

$$\sigma_c = \frac{P_{DL+LL}}{A_0} \leq 80 \text{ kgf/cm}^2 = 7.84 \text{ MN/m}^2 \tag{17.9}$$

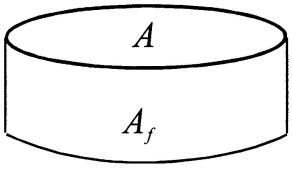

FIGURE 17.8 Load-free area A_f.

TABLE 17.1 Relation of Rubber Hardness and Material Constants

Rubber Hardness IRHD ±2	Young's Modulus E (N/cm^2)	Shear Modulus G (N/cm^2)	Modified Factor k
30	92	30	0.93
35	118	37	0.89
40	150	45	0.85
45	180	54	0.8
50	220	64	0.73
55	325	81	0.64
60	445	106	0.57
65	585	137	0.54
70	735	173	0.53
75	940	222	0.52

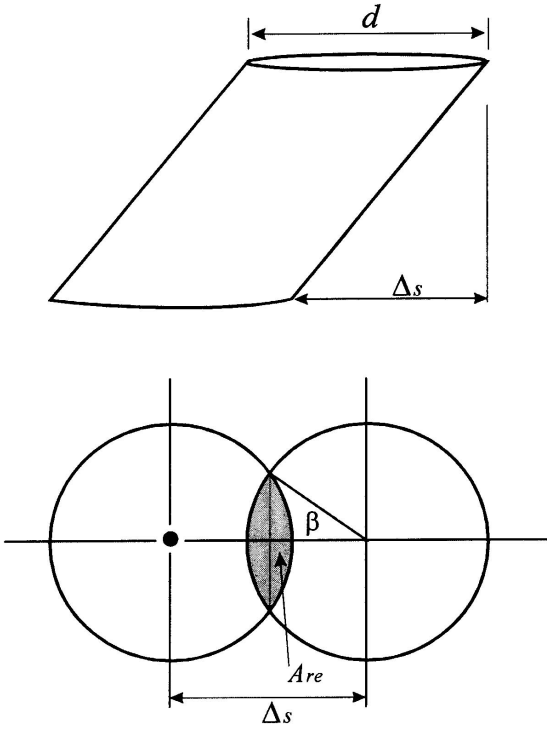

FIGURE 17.9 Reduced cross-sectional area of circular bearing.

c. Determine the effective cross-sectional area A_1 of the bearing from the shear strain due to the vertical load P_{DL+LL}:

$$\gamma_c\Big|_{DL+LL} = 6S\frac{P_{DL+LL}}{E_c A_1} \le \frac{\varepsilon_b}{3} \tag{17.10}$$

where ε_b is the elongation of rubber at break. The limit of $\varepsilon_b/3$ is selected according to the American Association of State Highway and Transportation Officials [1983] Guide Specifications.

d. Obtain the minimum cross-sectional area A_{sf} for shear failure of the bearing:

$$A_{sf} = \frac{K_{eff} \cdot t_r}{G} \tag{17.11}$$

Use A_{sf} to determine the dimensions of the bearing. Then compute the effective cross-sectional area A_2 as the reduced area A_{re} given below (see Figure 17.9 for circular bearings):

$$A_{re} = L \cdot \left(B - \Delta_S\right) \quad \text{for a rectangular bearing} \tag{17.12}$$

$$A_{re} = \frac{d^2}{4}\left(\beta - \sin\beta\right) \quad \text{for a circular bearing} \tag{17.13}$$

$$\beta = 2\cos^{-1}\left(\frac{\Delta_S}{d}\right) \tag{17.14}$$

where

L, B = plan dimensions of the bearing perpendicular and parallel to the displacement, respectively
Δ_s = horizontal displacement of the bearing

e. The design cross-sectional area A of the bearing is the maximum of the three values computed: A_0, A_1, and A_2.
f. Select proper dimensions for the rubber layer based on the design cross-sectional area A.

7. Single layer thickness, t, and number of rubber layers, N:
   a. Use the shape factor S and dimensions of the rubber layer to determine the thickness of individual rubber layer, t:

$$S = \frac{L \cdot B}{2(L+B) \cdot t} \quad \text{for a rectangular bearing} \tag{17.15}$$

$$S = \frac{\pi d^2/4}{\pi d t} = \frac{d}{4t} \quad \text{for a circular bearing} \tag{17.16}$$

where

L, B = plan dimensions of a rectangular bearing ($L \le B$)
d = diameter of a circular bearing
t = thickness of individual rubber layers

   b. Use $t_r = N \times t$ to determine the required number of rubber layers, N
8. Steel plate thickness, t_s:

$$t_s \ge \frac{2(t_i + t_{i+1}) \cdot P_{DL+LL}}{A_{re} \cdot F_S} \ge 2 \text{ mm} \tag{17.17}$$

where

t_i, t_{i+1} = rubber layer thickness in top and bottom of the steel plate
F_s = 0.6 F_y
F_y = yield strength of the steel plates (= 274.4 MN/m^2)
A_{re} = reduced cross-sectional area of the bearing under horizontal displacement

9. All the parameters determined for the bearing should be checked against the shear strain and stability conditions given below. If these requirements cannot be satisfied, then repeat steps 2 to 8 for an improved design.

17.5.2 Shear Strain and Stability Conditions for HDR Bearings

1. The rubber layers selected should satisfy the shear strain requirement under the vertical load P_{DL+LL}:

$$\gamma_{c,DL+LL} = 6S \cdot \varepsilon_c = 6S \cdot \frac{P_{DL+LL}}{E_c \cdot A} \le \frac{\varepsilon_b}{3} \tag{17.18}$$

where the compression strain ε_c is:

$$\varepsilon_c = \frac{\Delta_c}{t_r} = \frac{P_{DL+LL}}{E_c \cdot A} \tag{17.19}$$

Δ_c = compression displacement of the bearing

ε_b = elongation of rubber at break

2. Stability condition: To prevent the bearing from becoming unstable, the average compressive stress σ_c of the bearing should be less than a preset tolerance:

$$\sigma_c = \frac{P}{A} < \sigma_{cr} = \frac{G \cdot S \cdot L}{2.5 \cdot t_r} \tag{17.20}$$

where L is the least plan dimension of the rectangular bearing or the diameter d of the circular bearing. It should be noted that the following formulas were used by Naeim and Kelly [1999]:

$$\sigma_c = \frac{P}{A} < \sigma_{cr} = \begin{cases} \dfrac{\pi G \cdot S \cdot d}{2\sqrt{2} \cdot t_r} & \text{for a circular bearing} \\ \dfrac{\pi G \cdot S \cdot L}{\sqrt{6} \cdot t_r} & \text{for a rectangular bearing} \end{cases} \tag{17.21}$$

3. Shear strain condition for the earthquake load:

$$\gamma_{sc} + \gamma_{eq} + \gamma_{sr} \le 0.75\, \varepsilon_b \tag{17.22}$$

with

$$\gamma_{sc} = 6S \cdot \frac{P_{DL+LL+EQ}}{E_c \cdot A_{re}} \tag{17.23}$$

$$\gamma_{eq} = \frac{D}{t_r} \tag{17.24}$$

$$\gamma_{sr} = \frac{B^2 \cdot \theta}{2 \cdot t \cdot t_r} \tag{17.25}$$

$$\theta = \frac{12\,De}{b^2 + d^2} \tag{17.26}$$

where

γ_{sc} = shear strain under compression, same as in Equation 17.18, except that P_{DL+LL} is replaced by $P_{DL+LL+EQ}$
$P_{DL+LL+EQ}$ = combination of dead load, live load, and earthquake load
γ_{eq} = shear strain under earthquake
γ_{sr} = shear strain under rotation
θ = rotation angle of the bearing induced by earthquake
e = actual eccentricity + 5% of accidental eccentricity
b, d = dimensions of the structure with rectangular plan

4. To avoid rollout of the bearing, the displacement of the bearing under the earthquake load should fulfill the following condition:

$$D \le \delta_{roll\text{-}out} = \frac{P_{DL+LL+EQ} \cdot L}{P_{DL+LL+EQ} + K_{eff} \cdot h} \tag{17.27}$$

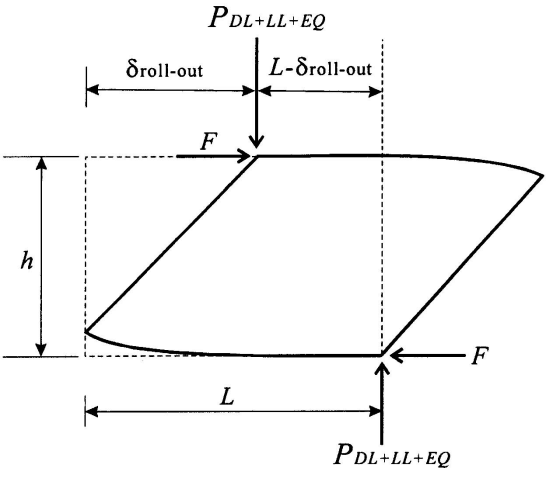

FIGURE 17.10 Bearing in rollout position.

where

K_{eff} = effective stiffness of the bearing
h = total height of the bearing (rubber plus steel)
L = least plan dimension of a rectangular bearing or diameter d of a circular bearing

Equation 17.27 can be derived from the following two equations established for the bearing in the deformed position, as shown in Figure 17.10:

$$F \cdot h = P_{DL+LL+EQ} \cdot \left(L - \delta_{roll\text{-}out}\right) \tag{17.28}$$

$$F = K_{eff} \cdot \delta_{roll\text{-}out} \tag{17.29}$$

where F is the shear force acting on the bearing and $\delta_{roll\text{-}out}$ the corresponding roll-out displacement.

17.6 Design of Lead Rubber Bearings

Lead rubber bearings (LRBs) are usually made of alternating layers of steel plates and natural rubber with a central hole into which the lead core is press-fitted. When subjected to lateral shear forces, the lead core deforms almost in pure shear, yields at low level of shear stresses, approximately 8 to 10 MPa at normal (20°C) temperature, and produces rather stable hysteretic deformation behavior over a number of cycles. One feature of the lead core is that it can recrystallize at normal temperature and will not encounter the problem of fatigue failure under cyclic loadings. Sufficient rigidity is always ensured by the LRBs for the structure under service loads. In this section, the design procedure for LRBs is outlined.

17.6.1 Design Procedure for Lead Rubber Bearings

The design procedure for LRBs is similar to that for HDRs, except that there is an additional need to design the lead core.

1. Specify the soil condition for the isolated structure.
2. Select the design shear strain γ_{max} and effective damping ratio ξ_{eff} for the bearing, and the target design period T_D for the isolated structure. The former can be obtained from the material supplier.
3. Use code formulas, or static or dynamic analysis to determine the effective horizontal stiffness K_{eff} and maximum horizontal (design) displacement D of the bearing.

4. Select the material properties, including Young's modulus E and shear modulus G, from the manufacturer's test report.
5. Calculate the total height of rubber layers, t_r, in the bearing according to the design displacement D and design shear strain γ_{max}:

$$t_r = \frac{D}{\gamma_{max}} \tag{17.30}$$

6. Lead core design: Determine the cross-sectional area A_p and diameter d_p of the lead core based on the short-term yield force Q_d and yield strength f_{py}:

$$A_p = \frac{Q_d}{f_{py}} \tag{17.31}$$

f_{py} = yield strength of the lead plug in shear = 1500 psi = 10 MPa [Mayes and Naeim, 2000]
Q_d = yield force of the lead plug $\cong W_D/(4D)$
W_D = energy dissipated per cycle = $2\pi K_{eff} D^2 \xi_{eff}$
D = design displacement of the bearing

7. Determine the area A and thickness t of individual rubber layers.
   a. Select the shape factor S under no rocking condition:

$$\frac{K_v}{K_h} = \frac{\dfrac{E_c \cdot A}{t_r}}{\dfrac{G \cdot A}{t_r}} = \frac{E_c}{G} = \frac{E \cdot \left(1 + 2\,kS^2\right)}{G} \geq 400 \tag{17.32}$$

   b. Compute the effective cross-sectional area A_0 of the bearing based on the allowable axial stress σ_c under the vertical load case P_{DL+LL}:

$$\sigma_c = \frac{P_{DL+LL}}{A_0} \leq 80 \text{ kgf/cm}^2 \;=\; 7.84 \text{ MN/m}^2 \tag{17.33}$$

   c. Determine the effective cross-sectional area A_1 of the bearing from the shear strain due to the vertical load P_{DL+LL}:

$$\gamma_c\Big|_{DL+LL} = 6S\frac{P_{DL+LL}}{E_c A_1} \leq \frac{\varepsilon_b}{3} \tag{17.34}$$

   d. Determine the elastic modulus K_r of the bearing:

$$K_d = K_r\left(1 + 12\frac{A_p}{A_0}\right) \tag{17.35}$$

where K_d = post-yield stiffness of the LRB in horizontal direction [Naeim and Kelly, 1999]:

$$K_d = K_{eff} - \frac{Q_d}{D} \tag{17.36}$$

e. Obtain the minimum cross-sectional area A_{sf} for shear failure of the bearing:

$$A_{sf} = \frac{K_r \cdot t_r}{G} \tag{17.37}$$

Use A_{sf} to determine the dimensions of the bearing. Then compute the effective cross-sectional area A_2 as the reduced area A_{re} given below:

$$A_{re} = L \cdot \left(B - \Delta_S\right) \quad \text{for a rectangular bearing} \tag{17.38}$$

$$A_{re} = \frac{d^2}{4}\left(\beta - \sin\beta\right) \quad \text{for a circular bearing} \tag{17.39}$$

f. The design cross-sectional area A of the bearing is the maximum among the three values computed: A_0, A_1, and A_2.

g. Select proper dimensions for the rubber layer based on the design area A.

8. Thickness of individual rubber layer, t, and the number of rubber layers, N:

a. Determine the thickness of individual rubber layer, t, from the shape factor S and dimensions of the rubber layer:

$$S = \frac{L \cdot B}{2\left(L + B\right) \cdot t} \quad \text{for a rectangular bearing} \tag{17.40}$$

$$S = \frac{d}{4t} \quad \text{for a circular bearing} \tag{17.41}$$

b. Use $t_r = N \times t$ to determine the required number of rubber layers, N.

9. Steel plate thickness, t_s:

$$t_s \geq \frac{2\left(t_i + t_{i+1}\right) \cdot P_{DL+LL}}{A_{re} \cdot F_S} \geq 2 \text{ mm} \tag{17.42}$$

where each parameter has been defined previously.

10. The shear strain and stability conditions are given in the section to follow. If the dimensions determined for the bearing cannot satisfy the shear strain and stability requirements, then repeat steps 2 to 9 for an improved design.

17.6.2 Shear Strain and Stability Checks

1. In the design of rubber layers, the following shear strain condition for the normal load case should be satisfied:

$$\gamma_{c,DL+LL} = 6S \cdot \varepsilon_c = 6S \cdot \frac{P_{DL+LL}}{E_c \cdot A} \leq \frac{\varepsilon_b}{3} \tag{17.43}$$

where all the parameters have been defined following Equation 17.18.

2. Stability condition: To prevent the bearing from becoming unstable, the average compression stress σ_c of the bearing should fulfill the following condition:

$$\sigma_c = \frac{P}{A} < \sigma_{cr} = \frac{G \cdot S \cdot L}{2.5 \cdot t_r} \tag{17.44}$$

where it should be noted that L is the least dimension of a rectangular bearing or the diameter d of a circular bearing.

3. Lead core size: The lead core provides the initial stiffness and energy dissipation capability to the bearing, whose dimensions should meet the following condition:

$$1.25 \le \frac{H_p}{d_p} \le 5.0 \tag{17.45}$$

where

H_p = effective height of the lead core
d_p = diameter of the lead core

4. Load combination including the earthquake:

$$\gamma_{sc} + \gamma_{eq} + \gamma_{sr} \le 0.75\varepsilon_b \tag{17.46}$$

where all the parameters have been defined following Equation 17.22.

5. To protect the bearing from the occurrence of rollout, the displacement D of the bearing under the earthquake load should fulfill the following condition:

$$D \le \delta_{roll\text{-}out} = \frac{P_{DL+LL+EQ} \cdot L}{P_{DL+LL+EQ} + K_d \cdot h} \tag{17.47}$$

where K_d indicates the post-yield stiffness of the bearing in the horizontal direction.

17.7 Design of Friction Pendulum Systems

The frictional pendulum bearing allows the supported structure to return to its original position through use of a spherical concave sliding surface, rather than a flat sliding surface, thereby conquering the problem of recentering. Since the frictional pendulum bearing allows the isolated structure to vibrate in a way similar to the pendulum, it implies a natural period of vibration, T_D. In design of the frictional pendulum bearing, one key concern is to make the natural period T_D long enough, such that the forces transmitted from the ground to the superstructure can be greatly reduced. The period T_D of the friction pendulum system (FPS) isolated structure can be designed through a proper choice of the radius of curvature, R_{FPS}, for the spherical sliding surface, that is,

$$T_D = 2\pi\sqrt{\frac{R_{FPS}}{g}} \tag{17.48}$$

where g is the acceleration of gravity. As can be seen from Equation 17.48, the period of the FPS is independent of the mass of the supported structure. Such a property represents an advantage of the FPS in controlling the response of the isolated structure. Because of the use of a concave sliding surface, the FPS provides a recentering mechanism for the isolated structure to return to its original position after earthquake shaking. Let the vertical load carried by each FPS at the column base be W. The effective stiffness of the FPS is:

$$K_{eff} = \frac{W}{R_{FPS}} + \frac{\mu W}{D} \tag{17.49}$$

where μ is the frictional coefficient of the sliding surface and D the design displacement. As indicated by Equation 17.49, the effective stiffness K_{eff} of the FPS depends on the supported load W, which makes it difficult for designers to select suitable isolation systems for columns with different sustained loads. The effective damping ratio ξ_{eff} provided by the isolation system is a function of the design displacement, which can be expressed as:

$$\xi_{eff} = \frac{2}{\pi} \frac{\mu}{\mu + D/R_{FPS}} \tag{17.50}$$

The vertical displacement δ_v of the structure caused by the curved surface of the isolator can be estimated as:

$$\delta_v \cong \frac{D^2}{2R_{FPS}} \tag{17.51}$$

To ensure that the isolated structure will return to its original position, the horizontal displacement D of the structure under the earthquake load should meet the requirement that the restoring force F ($= WD/R_{FPS}$) is not less than the friction force μW, that is:

$$\frac{D}{R_{FPS}} \geq \mu \tag{17.52}$$

This is exactly the condition to be checked for recentering of the isolated structure.

17.8 Design Examples

A three-story reinforced concrete shear-wall office building is located on a rock site, i.e., site class B, and far away from active faults. If the building is constructed with a fixed base, the reduction factor is $R = 6$. According to Section 1623.2.5.2 of the IBC [ICC, 2000], if the building is base isolated, the reduction factor R_I should be modified as:

$$1.0 \leq R_I = \frac{3}{8} R \leq 2.0$$

For all the isolation cases to be presented, the reduction factor is taken as $R_I = 2$. The plan of the building is given in Figure 17.11. The story heights are 5 m for the first story and 4 m for the second and third stories. The sizes of the columns, beams, walls, and slabs are given as follows:

Interior column C_1:	0.30×0.30 m
Exterior column C_2:	0.25×0.25 m
Beams B, G:	0.25×0.40 m
Equivalent wall W_1 thickness:	0.08 m
Slab thickness S:	0.15 m

The story loads on the building are: dead load = 10 kN/m^2 and live load = 2.5 kN/m^2. The building has a regular plan with three columns spaced at 6 m along the x direction, and also three columns at 4 m apart along the y direction, as shown in Figure 17.11. The total weight W_T of the building is 5,209 kN. Due to the limitation of site boundaries, the allowable horizontal displacement of the building at the base is 30 cm. By a static analysis using the ETABS program [CSI, 1997], the loads computed for all the columns at their base, where the bearings are to be installed, are shown in Figure 17.12. The natural periods of vibration for the fixed-base building along the x and y directions are 0.24 and 0.16 sec, respectively.

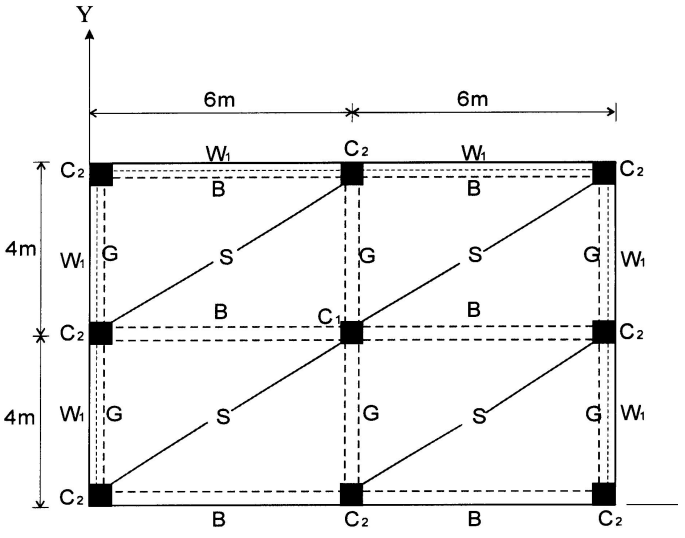

FIGURE 17.11 Plan of three-story building.

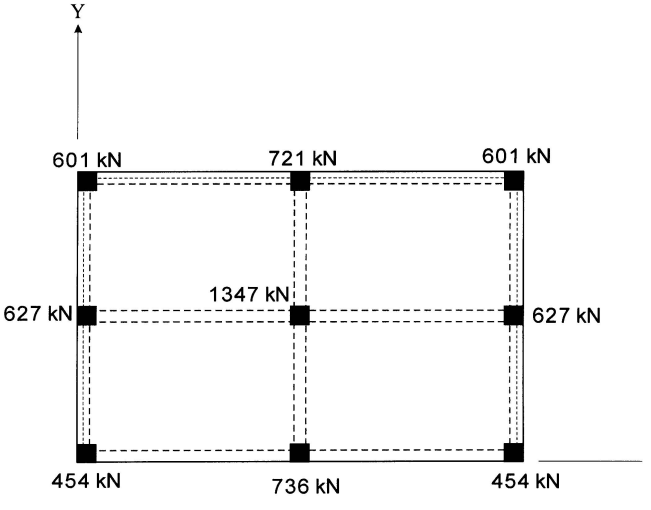

FIGURE 17.12 Column loads of the building.

For the purpose of illustration, only the design of one bearing is considered. This is the one that will be installed at the base of the interior (central) column, of which the maximum sustained load is P_{DL+LL} = 1,347 kN = 1.347 MN.

17.8.1 High Damping Rubber Bearings

For this example, the design target period T_D of the isolated structure should be greater than three times the fixed-base period. Let us assume that: (1) the target period T_D = 2.5 sec, (2) the laminated rubber bearing has a maximum shear strain γ_{max} = 150%, and (3) the effective damping ratio is ξ_{eff} = 20%. From Table 1623.2.2.1 of the IBC 2000, for an isolation system with ξ_{eff} = 20%, the damping coefficient B_D is 1.5. From Table 1615.1.2(2) of the same code, for the site of the isolated building with long periods, the seismic coefficient is S_D = 0.4.

17.8.1.1 Analysis

The effective horizontal stiffness K_{eff} of the isolator is:

$$K_{eff} = \frac{W}{g}\left(\frac{2\pi}{T_D}\right)^2\Bigg|_{W=P_{DL+LL}} = \frac{1347}{9.8}\left(\frac{2\pi}{2.5}\right)^2 = 868\ \text{kN/m} = 0.868\ \text{MN/m}$$

Based on Equation 16-79 of IBC 2000, the design displacement D_D is:

$$D_D = \left(\frac{g}{4\pi^2}\right)\frac{S_D T_D}{B_D} = \frac{9.8}{4\pi^2}\times\frac{0.4\times 2.5}{1.5} = 0.17\ \text{m} \le 0.3\ \text{m} \rightarrow \text{OK}$$

17.8.1.2 Design

1. Determine the isolator size.
   1.1 The total rubber height
   $t_r = D_D/\gamma_{max} = 0.17/1.5 = 0.11$ m
   Use $t_r = 0.12$ m.
   1.2 Select the rubber properties from Table 17.1. Use the following for the rubber: hardness = IRHD-60, elongation at break $\varepsilon_b = 500\%$. The material properties are obtained as follows:
   $E = 445\ \text{N/cm}^2 = 4.45\ \text{MN/m}^2$
   $G = 106\ \text{N/cm}^2 = 1.06\ \text{MN/m}^2$
   $k = 0.57$
   1.3 Calculate the area A and thickness t of individual rubber layers.
   a. Select the shape factor S:

$$\frac{E\cdot\left(1+2kS^2\right)}{G} \ge 400 \rightarrow \frac{445\cdot\left(1+2\times 0.57S^2\right)}{106} \ge 400$$

$$\rightarrow S > 9.09 \rightarrow \text{Use } S = 20$$

$$E_c = E\cdot\left(1+2kS^2\right) = 445\cdot\left(1+2\times 0.57\times 20^2\right) = 203365\,\text{N/cm}^2$$

$$= 2033.65\,\text{MN/m}^2$$

   b. Determine the effective area A_0 for the bearing based on the allowable axial stress σ_c for the vertical load case P_{DL+LL}:

$$\sigma_c = \frac{P_{DL+LL}}{A_0} \le 7.84\,\text{MN/m}^2 \rightarrow \frac{1.347\,\text{kN}}{A_0} \le 7.84\ \text{MN/m}^2$$

$$\rightarrow A_0 > 0.172\,\text{m}^2$$

   c. Determine the effective area A_1 for the bearing from the shear strain condition under the vertical load case P_{DL+LL}:

$$6S = \frac{P_{DL+LL}}{E_c\cdot A_1} \le \frac{\varepsilon_b}{3} \rightarrow 6\times 20\times\frac{1.347}{2033.65\times A_1} \le \frac{500\%}{3}$$

$$\rightarrow A_1 > 0.048\,\text{m}^2$$

d. Obtain the minimum area A_{sf} for shear failure of the bearing:

$$G = \frac{K_{eff} \cdot t_r}{A_{sf}} \rightarrow A_{sf} = \frac{K_{eff} \cdot t_r}{G} = \frac{0.868 \times 0.12}{1.06} = 0.098\,\text{m}^2$$

For a circular bearing, the diameter corresponding to the area A_{sf} is $d = 0.35$ m. It follows that the effective area can be computed from Equations 17.13 and 17.14 as $A_2 = 0.039$ m^2.

e. The design cross-sectional area for the bearing is:

$$A = \max(A_0, A_1, A_2) = \max(0.172, 0.048, 0.039) = 0.172 \text{ m}^2$$

f. Determine the size of rubber layers: Use the following equations for a circular bearing:

$$A_{re} \le \frac{d^2}{4}(\beta - \sin\beta)$$

$$\beta = 2\cos^{-1}\left(\frac{D_D}{d}\right)$$

$\rightarrow$ Diameter $d = 0.7$ m, area $A = 0.385$ m^2, reduced area $A_{re} = 0.267$ m^2

g. Single layer thickness, t, and number of layers, N: For a circular bearing:

$$S = \frac{d}{4t} \rightarrow 20 = \frac{70}{4t} \rightarrow t = 0.88 \text{ cm; use } t = 1 \text{ cm}$$

1.4 Determine the steel plate thickness, t_s:

$$t_s \ge \frac{2(t_i + t_{i+1}) \cdot P_{DL+LL}}{A_{re} \cdot F_S} \ge 2 \text{ mm}$$

$$t_s \ge \frac{2 \cdot (0.01 + 0.01) \times 1.347}{0.267 \times (0.6 \times 274.4)} = 0.0012 \text{ m} = 1.2 \text{ mm}$$

Use $t_s = 2$ mm

where, for A36 steel:

$$F_s = 0.6F_y = 0.6 \times 274.4 \text{ MN/m}^2$$
$$A_{re} = 0.267 \text{ m}^2, \beta = 2 \times \cos^{-1}(0.17/0.7)$$

1.5 Total height h of the bearing: Assume both the top and bottom cover plates are 2.5 cm thick. The total height of the bearing is:

$$h = t_r + 11 \times t_s + 2 \times 2.5 \text{ cm} = 12 \text{ cm} + 11 \times 2 \text{ mm} + 5 \text{ cm} = 19.2 \text{ cm}$$

2. Shear strain and stability conditions

2.1 Vertical load P_{DL+LL}\:

$$\gamma_{c,DL+LL} = 6S \cdot \frac{P_{DL+LL}}{E_c \cdot A} = 6 \times 20 \times \frac{1.347}{2033.65 \times 0.385} = 0.206$$

$$\le \frac{\varepsilon_b}{3} = \frac{500\%}{3} = 1.667 \rightarrow \text{OK}$$

2.2 Stability check:

$$\sigma_c = \frac{P}{A} = \frac{1347}{0.385} = 3500\,\text{kN/m}^2$$

$$\leq \sigma_c = \frac{G \cdot S \cdot L}{2.5 \cdot t_r} = \frac{(1.06 \times 10^3) \times 20 \times 0.7}{2.5 \times 0.12} = 49467\ \text{kN/m}^2 \rightarrow \text{OK}$$

3. Design result: dimensions of the HDR:
   Diameter of the bearing, d = 70 cm
   Total height of the bearing, h = 19.2 cm
   Number of rubber layers, N = 12
   Thickness of individual layers, t = 1 cm
   Number of steel plates, N_s = 11
   Thickness of individual plates, t_s = 2 mm
   Thickness of top and bottom cover plates = 2.5 cm
4. Earthquake response analysis:
   4.1 Structural periods obtained from dynamic analysis by ETABS [CSI, 1997]:
   T_{Dpx} = 1.71 sec
   T_{Dpy} = 1.67 sec
   4.2 Minimum base shear V_b at the isolation interface:

$$V_{b,1} = K_H \times D_D = \left(\sum K_{eff}\right) \times D_D = (868 \times 9) \times 0.17 = 1328\ \text{kN}$$

$$V_{b,2} = \frac{W_T}{g}\left(\frac{2\pi}{T_{Dp}}\right)^2 \times D_D = \frac{5209}{9.81}\left(\frac{2\pi}{1.67}\right)^2 \times 0.17 = 1278\ \text{kN}$$

$$V_b = \max\left(V_{b,1}, V_{b,2}\right) = 1328\ \text{kN}$$

Design earthquake force of the superstructure above the isolation interface:

$$V_s = V_b/R_I = 1328/2 = 664\ \text{kN} = 0.128\ W_T$$

where the reduction factor R_I is equal to 2 for all the isolation cases, as was mentioned previously. It must be noted that the design shear force V_s should be greater than the base shear of the fixed-base structure situated at the same site with a target period of 2.5 sec.

4.3 Vertical distribution of design earthquake forces: The lateral force F_x acting at level x of the isolated structure can be computed from the base shear force V_s by:

$$F_x = \frac{w_x h_x}{\sum_{i=1}^{N} w_i h_i} \times V_s$$

where w_x and w_i are the weights at levels x and i, respectively, h_x and h_i are the respective heights of the structure above the isolation interface. By the preceding formula, the lateral forces computed for levels RF, 3F, and 2F are 320, 221, and 123 kN, respectively. The lateral force at level 1F is 1328 kN. By considering 5% of accidental eccentricity of the building dimensions, and by applying simultaneously 100% of the vertical and horizontal loads for the x direction and 30% of the horizontal loads for the y direction, the maximum compression force computed by the ETABS [CSI, 1997] program for the central isolator under the earthquake load $P_{DL+LL+EQ}$ is 1387 kN. Moreover, the drift ratios computed for levels RF, 3F, and 2F are 0.263%, 0.265%, and 0.261%, indicating that the isolated structure behaves like a rigid body under the earthquake motions.

5. Checks on stability and rollout under the earthquake load:
   5.1 Shear strain condition including the earthquake effect:

$$P_{DL+LL+EQ} = 1387 \text{ kN} = 1.387 \text{ MN}$$

$$\gamma_{sc} = 6S \cdot \frac{P_{DL+LL+EQ}}{A_{re} \cdot E_c} = 6 \times 20 \times \frac{1.387}{0.267 \times 2033.65} = 0.307$$

$$\gamma_{eq} = D / t_r = 0.17 / 0.12 = 1.417$$

$$\theta = \frac{12 D_D \times e}{b^2 + d^2} = \frac{12 \times 0.17 \times (0.05 \times 12)}{12^2 + 8^2} = 0.006$$

$$\gamma_{sr} = \frac{B^2 \cdot \theta}{2 \cdot t \cdot t_r} = \frac{70^2 \times 0.006}{2 \times 1 \times 12} = 1.225$$

(Here B is interpreted as the diameter d for circular bearings):

$$\gamma_{sc} + \gamma_{eq} + \gamma_{sr} = 0.307 + 1.417 + 1.225 = 2.95$$
$$< 0.75 \varepsilon_b = 0.75 \times 500\% = 3.75 \rightarrow \text{OK}$$

   5.2 Rollout condition:

$$\delta_{roll-out} = \frac{1}{2} \times \frac{P_{DL+LL+EQ} \cdot L}{P_{DL+LL+EQ} + K_{eff} \cdot h} = \frac{1}{2} \times \frac{1387 \times 0.7}{1387 + 868 \times 0.192}$$
$$= 0.31 \text{ m} = 31 \text{ cm} > D_D = 17 \text{ cm} \rightarrow \text{OK}$$

(Here L is interpreted as the diameter d for circular bearings)

17.8.2 Lead Rubber Bearings

Assume the following for the isolated structure with LRBs: (1) the design target period T_D = 2.5 sec; (2) the laminated rubber bearing has a maximum shear strain of γ_{max} = 50%; and (3) the effective damping ratio is ξ_{eff} = 10%. From Table 1623.2.2.1 of IBC 2000, the damping coefficient B_D corresponding to the effective damping of ξ_{eff} = 10% for the LRB isolation system is 1.2. For the site condition of the isolated building with long period, the seismic coefficient is taken as S_D = 0.4.

17.8.2.1 Analysis

The effective horizontal stiffness of the isolator is:

$$K_{eff} = \frac{W}{g}\left(\frac{2\pi}{T_D}\right)^2\Bigg|_{W=P_{DL+LL}} = \frac{1347}{9.8}\left(\frac{2\pi}{2.5}\right)^2 = 868 \text{ kN/m} = 0.868 \text{ MN/m}$$

The design displacement D_D is:

$$D_D = \left(\frac{g}{4\pi^2}\right)\frac{S_D T_D}{B_D} = \frac{9.8}{4\pi^2} \times \frac{0.4 \times 2.5}{1.2} = 0.21 \text{ m} \le 0.3 \text{ m} \rightarrow \text{OK}$$

The short term yield force Q_d is:

$$Q_d = \frac{W_D}{4D_D} = \frac{\pi}{2} K_{eff} \xi_{eff} D_D = \frac{\pi}{2} \times 868 \times 10\% \times 0.21 = 28.6 \text{ kN}$$

The post-yield horizontal stiffness K_d is:

$$K_d = K_{eff} - \frac{Q_d}{D_D} = 868 - \frac{28.6}{0.21} = 773 \text{ kN}$$

17.8.2.2 Design

1. Design lead core: Assume the yield strength of the lead core to be $f_{py} = 8.82$ MN/m^2. The required lead area is:

$$A_p = \frac{Q_d}{f_{py}} = \frac{28.6}{8.82 \times 10^3} = 0.325 \times 10^{-2} \text{m}^2 = 32.5 \text{ cm}^2$$

   Use diameter $d_p = 7$ cm.

2. Design the area and dimensions of rubber layers:

   2.1 Total height of rubber layers:

$$t_r = D_D/\gamma_{\max} = 0.21/0.5 = 0.42 \text{ m}$$

   2.2 Select the rubber properties from Table 17.1. Assume the rubber hardness to be IRHD-60 and the elongation of rubber at break is $\varepsilon_b = 500\%$. The material properties obtained from Table 17.1 are:

$E = 445$ N/cm^2 = 4.45 MN/m^2
$G = 106$ N/cm^2 = 1.06 MN/m^2
$k = 0.57$

   2.3 Select the shape factor, S:

$$\frac{E \cdot \left(1 + 2kS^2\right)}{G} \geq 400 \rightarrow \frac{445 \cdot \left(1 + 2 \times 0.57 S^2\right)}{106} \geq 400$$

$$\rightarrow S > 9.09 \rightarrow \text{Use } S = 20$$

$$E_c = E \cdot \left(1 + 2kS^2\right) = 445 \cdot \left(1 + 2 \times 0.57 \times 20^2\right) = 203365 \text{ N/cm}^2$$

$$= 2033.65 \text{ MN/m}^2$$

   2.4 Determine the effective area A_0 of the bearing based on the allowable normal stress σ_c under the vertical load case P_{DL+LL}:

$$\sigma_c = \frac{P_{DL+LL}}{A_0} \leq 7.84 \text{ MN/m}^2 \rightarrow \frac{1347 \text{kN}}{A_0} \leq 7.84 \text{ MN/m}^2$$

$$\rightarrow A_0 > 0.172 \text{ m}^2$$

   2.5 Determine the effective area A_1 from the shear strain condition for the vertical load case P_{DL+LL}:

$$6S \frac{P_{DL+LL}}{E_c \cdot A_1} \leq \frac{\varepsilon_b}{3} \rightarrow 6 \times 20 \times \frac{1.347}{2033.65 \times A_1} \leq \frac{500\%}{3}$$

$$\rightarrow A_1 > 0.048 \text{m}^2$$

   2.6 Elastic stiffness K_r of the bearing:

$$K_d = K_r \left(1 + 12 \frac{A_p}{A_0}\right) \rightarrow 773 = K_r \left(1 + 12 \times \frac{127}{1720}\right)$$

$$\rightarrow K_r = 630 \text{ kN/m}$$

2.7 Determine the effective area A of individual rubber layers based on shear failure condition:

$$G = \frac{K_r \cdot t_r}{A_{sf}} \rightarrow A_{sf} = \frac{K_r \cdot t_r}{G} = \frac{630 \times 0.42}{1.06 \times 10^3} = 0.250 \text{ m}^2$$

For a circular bearing, the diameter corresponding to the area A_{sf} is $d = 0.56$ m. It follows that the effective area can be computed from Equation 17.39 as $A_2 = 0.132$ m^2:

$$A = \max(A_0, A_1, A_2) = \max(0.172, 0.048, 0.132) = 0.172 \text{ m}^2$$

2.8 Determine the size and dimensions of rubber layers. For circular bearings:

$$A_{re} \le \frac{d^2}{4}(\beta - \sin\beta)$$

$$\beta = 2\cos^{-1}\left(\frac{D_D}{d}\right)$$

$\rightarrow$ Diameter $d = 0.7$ m, area $A = 0.385$ m^2, reduced area $A_{re} = 0.267$ m^2

2.9 Single layer thickness, t, and number of layers, N. For circular bearing:

$$S = \frac{d}{4t} \rightarrow 20 = \frac{70}{4t} \rightarrow t = 0.88 \text{ cm}; \text{ use } t = 1 \text{ cm}$$

$$t_r = N \times t \rightarrow 42 = N \times 1 \rightarrow N = 42$$

Use $N = 42$.

2.10 Steel plate thickness t_s:

$$t_s \ge \frac{2(t_i + t_{i+1}) \cdot P_{DL+LL}}{A_{re} \cdot F_S}$$

$$t_s \ge \frac{2 \cdot (0.01 + 0.01) \times 1.347}{0.267 \times (0.6 \times 274.4)} = 0.0012 \text{ m} = 1.2 \text{ mm}$$

Use $t_s = 2$ mm.

where, for A36 steel, $F_s = 0.6F_y = 0.6 \times 274.4$ MN/m^2 = 164.6 MN/m^2:

$$A_{re} = 0.267 \text{ m}^2, \beta = 2 \times \cos^{-1}(0.17/0.7)$$

2.11 Total height h of the bearing. Assume the thickness of the top and bottom cover plates both to be 2.5 cm. The total height is:

$$h = t_r + 41 \times t_s + 2 \times 2.5 \text{ cm} = 42 \text{ cm} + 41 \times 2 \text{ mm} + 5 \text{ cm} = 55.2 \text{ cm}$$

3. Shear strain and stability conditions:

3.1 Vertical load P_{DL+LL}:

$$\gamma_{sc,DL+LL} = 6S \cdot \frac{P_{DL+LL}}{E_c \cdot A} = 6 \times 20 \times \frac{1.347}{2033.65 \times 0.385} = 0.206$$

$$\le \frac{\varepsilon_b}{3} = \frac{500\%}{3} = 1.667 \rightarrow \text{OK}$$

3.2 Stability check:

$$\sigma_c = \frac{P}{A} = \frac{1347}{0.385} = 3498 \text{ kN/m}^2$$

$$\leq \sigma_c = \frac{G \cdot S \cdot L}{2.5 \cdot t_r} = \frac{(1.06 \times 10^3) \times 20 \times 0.7}{2.5 \times 0.42} = 14{,}133 \text{ kN/m}^2 \rightarrow \text{OK}$$

3.3 Check on diameter of the lead core:

$$1.25 \leq \frac{H_p}{d_p} = \frac{42}{13} = 3.23 \leq 5.0 \rightarrow \text{OK}$$

4. Design result: dimensions of LRB:
   Diameter of the bearing, d = 70 cm
   Total height of the bearing, h = 55.2 cm
   Number of rubber layers, N = 42
   Thickness of individual layers, t = 1 cm
   Diameter of the lead core, d_p = 13 cm
   Number of steel plates, N_s = 41
   Thickness of steel plates, t_s = 2 mm
   Thickness of top and bottom cover plates = 2.5 cm
5. Earthquake response analysis:
   5.1 Structural periods obtained from dynamic analysis by ETABS [CSI, 1997]:
   T_{Dpx} = 1.71 sec
   T_{Dpy} = 1.67 sec
   5.2 Minimum base shear V_b at the isolation interface:

$$V_{b,1} = K_H \times D_D = \left(\sum K_{eff}\right) \times D_D = (868 \times 9) \times 0.21 = 1{,}641 \text{ kN}$$

$$V_{b,2} = \frac{W_T}{g}\left(\frac{2\pi}{T_{Dp}}\right)^2 \times D_D = \frac{5209}{9.81}\left(\frac{2\pi}{1.67}\right)^2 \times 0.21 = 1{,}578 \text{ kN}$$

$$V_b = \max\,(V_{b,1}, V_{b,2}) = 1{,}641 \text{ kN}$$

Design earthquake force of the superstructure above the isolation interface

$$V_s = V_b/R_I = 1641/2 = 820 \text{ kN} = 0.157\ W_T$$

where R_I = 2 has been used.

5.3 Vertical distribution of design earthquake forces. The lateral force F_x acting at level x of the isolated structure can be computed using the equation given below:

$$F_x = \frac{w_x h_x}{\sum_{i=1}^{N} w_i h_i} \times V_s$$

where all the parameters are defined as those given previously. The lateral forces computed for levels RF, 3F, and 2F are 395, 273, and 152 kN, respectively. The lateral force for level 1F is 1641 kN. By considering 5% of accidental eccentricity of the building dimensions, and by applying simultaneously 100% of the vertical and horizontal loads for the x direction and

30% of the horizontal loads for the *y* direction, the maximum compression force computed by the ETABS [CSI, 1997] program for the central isolator under the earthquake load $P_{DL+LL+EQ}$ is 1554 kN. The drift ratios computed for levels RF, 3F, and 2F are 0.325%, 0.327%, and 0.322%, indicating that the superstructure behaves essentially like a rigid body.

6. Checks on stability and rollout conditions under the earthquake load:

   6.1 Shear strain condition for the earthquake load:

$$P_{DL+LL+EQ} = 1554 \text{ kN} = 1.554 \text{ MN}$$

$$\gamma_{sc} = 6S \cdot \frac{P_{DL+LL+EQ}}{A_{re} \cdot E_c} = 6 \times 20 \times \frac{1.554}{0.267 \times 2033.65} = 0.343$$

$$\gamma_{eq} = D / t_r = 21 / 42 = 0.5$$

$$\theta = \frac{12 D_D \times e}{b^2 + d^2} = \frac{12 \times 0.17 \times (0.05 \times 12)}{12^2 + 8^2} = 0.006$$

$$\gamma_{sr} = \frac{B^2 \cdot \theta}{2 \cdot t \cdot t_r} = \frac{70^2 \times 0.006}{2 \times 1 \times 42} = 0.35$$

$$\gamma_{sc} + \gamma_{eq} + \gamma_{sr} = 0.34 + 0.5 + 0.35 = 1.19$$

$$< 0.75\, \varepsilon_b = 0.75 \times 500\% = 3.75 \rightarrow \text{OK}$$

   6.2 Rollout condition:

$$\delta_{roll\text{-}out} = \frac{1}{2} \times \frac{P_{DL+LL+EQ} \cdot L - Q_d \cdot h}{P_{DL+LL+EQ} + K_d \cdot h} = \frac{1}{2} \times \frac{1554 \times 0.7 - 28.6 \times 0.552}{1554 + 773 \times 0.552}$$

$$= 0.27 \text{ m} = 27 \text{ cm} > D_D = 21 \text{ cm} \rightarrow \text{OK}$$

17.8.3 Frictional Pendulum Systems

Use the same target period of T_D = 2.5 sec for the FPS isolated structure. Let the friction coefficient of the spherical sliding surface of the FPS be 0.06 and the design horizontal displacement *D* be 20 cm.

1. Determine the size of the FPS. The radius of curvature of the spherical sliding surface of the isolator is:

$$R_{FPS} = g\left(\frac{T_D}{2\pi}\right)^2 = 9.8\left(\frac{2.5}{2\pi}\right)^2 = 1.55 \text{ m; use } R_{FPS} = 1.5 \text{ m}$$

2. The total effective stiffness of the isolation system is given by:

$$\sum K_{eff} = \frac{W_T}{R_{FPS}} + \frac{\mu W_T}{D} = \frac{5209}{1.5} + \frac{0.06 \times 5209}{0.2} = 5{,}035 \text{ kN/m}$$

   Thus, the average effective stiffness K_{eff} for a single FPS isolator is 5,035/9 = 560 kN/m.

3. The effective damping ξ_{eff} provided by the isolator depends on the design displacement *D*, which can be computed as:

$$\xi_{eff} = \frac{2}{\pi} \frac{\mu}{\mu + D/R} = \frac{2}{\pi} \frac{0.06}{0.06 + 0.2/1.5} = 0.20 = 20\%$$

From Table 1623.2.2.1 of IBC 2000, the damping coefficient B_D corresponding to ξ_{eff} = 20% for the FPS isolation system is found to be 1.5. For the site condition of the isolated building with long period, the seismic coefficient is taken as S_D = 0.4.

4. Check the design displacement D_D:

$$D_D = \left(\frac{g}{4\pi^2}\right)\frac{S_D T_D}{B_D} = \frac{9.8}{4\pi^2} \times \frac{0.4 \times 2.5}{1.5} = 0.17 \text{ m} \le D = 0.2 \text{ m} \rightarrow \text{OK}$$

5. Estimate of the vertical displacement δ_v:

$$\delta_v \cong \frac{D^2}{2R_{FPS}} = \frac{0.2^2}{2 \times 1.5} = 0.013 \text{ m} = 1.3 \text{ cm}$$

Use depth δ = 1.7 cm for the disk.
Use diameter d = 45 cm for the disk of the FPS (> 2D).

$$\text{Check: } \frac{(d/2)^2}{2 \times R_{FPS}} = \frac{(0.45/2)^2}{2 \times 1.5} = 0.017 \text{ m} \ge 0.013 \text{ m} \rightarrow \text{OK}$$

6. Check on the recentering condition for the earthquake load case:

$$\frac{D}{R_{FPS}} = \frac{0.2}{1.5} = 0.13 \ge \mu = 0.06$$
$$\rightarrow \text{ OK}$$

7. Dimensions for the FPS:
   Radius of curvature of the spherical surface, R_{FPS} = 1.5 m
   Depth of the disk, δ = 1.7 cm
   Diameter of the disk, d = 45 cm
8. Earthquake response analysis:
   8.1 Structural periods obtained from dynamic analysis by ETABS [CSI, 1997]:
   T_{Dpx} = 2.042 sec
   T_{Dpy} = 2.036 sec
   8.2 Minimum base shear V_b of the isolated building at the isolation interface:

$$V_{b,1} = K_H \times D = \left(\sum K_{eff}\right) \times D = 5035 \times 0.2 = 1{,}007 \text{ kN}$$

$$V_{b,2} = \frac{W_T}{g}\left(\frac{2\pi}{T_{Dp}}\right)^2 \times D = \frac{5209}{9.81}\left(\frac{2\pi}{2.036}\right)^2 \times 0.2 = 1{,}012 \text{ kN}$$

$$V_b = \max(V_{b,1}, V_{b,2}) = 1{,}012 \text{ kN}$$

Design earthquake force of the superstructure above the isolation interface:

$$V_s = V_b/R_I = 1012/2 = 506 \text{ kN} = 0.097 \, W_T$$

where R_I = 2 has been used.

8.3 Vertical distribution of design earthquake forces. The lateral force F_x acting at level x of the isolated structure can be computed according to the following equation:

$$F_x = \frac{w_x h_x}{\sum_{i=1}^{N} w_i h_i} \times V_s$$

where all parameters have been defined before. Using the preceding formula, the lateral forces computed for levels RF, 3F, and 2F are 244, 168, and 94 kN, respectively. The lateral force at level 1F is 1012 kN. By considering 5% of accidental eccentricity of the building and by applying simultaneously 100% of the vertical and horizontal loads for the x direction and 30% of the horizontal loads for the y direction, the minimum and maximum compression forces computed by the ETABS [CSI, 1997] program for the isolators under the earthquake load $P_{DL+LL+EQ}$ are 74 kN and 1410 kN, respectively. This result indicates that all the FPSs are subjected to the action of compressive forces, ensuring that the effect of friction can be developed. The drift ratios computed for levels RF, 3F, and 2F are 0.024%, 0.024%, and 0.019%, respectively, indicating that the superstructure can be essentially regarded as a rigid body.

17.9 Concluding Remarks

While the application of various isolation devices for building construction has increased rapidly in recent years, the concept of seismic isolation is not a new one. Nowadays, many new materials and devices continue to be proposed for use in base isolation. The procedures presented in this chapter serve merely to illustrate the key concepts involved in initial sizing of the base isolation systems. It is the duty of the designer to make sure that the principles introduced herein are not violated by the specific isolators selected for their projects. For devices that tend to elongate the period of the protected structure, it is important to make sure that the structure is not located on a site with soft soils. For structures that are situated on soft soils or are of relatively long periods, only devices with energy dissipation mechanisms should be used. Compared with new construction, extra care must be taken in applying isolators to the rehabilitation of existing buildings, as there may exist additional restraints (historical, architectural, or other reasons) concerning the selection and installation of isolators.

References

American Association of State Highway and Transportation Officials (AASHTO), 1983. *Guide Specifications for Seismic Design of Highway Bridges*, Washington, D.C.

Bridgestone Corporation, 1990. *Multi-Rubber Bearings*, International Industrial Products Department, Tokyo.

Chopra, A.K., 1995. *Dynamics of Structures*, Prentice-Hall, Englewood Cliffs, NJ.

Computers and Structures, Inc. (CSI), 1997. *ETABS Version 6.2: Three-Dimensional Building Systems*, Berkeley, CA.

Dynamic Isolation System, Inc., 1990. *Force Control Bearings for Bridges*, Berkeley, CA.

Earthquake Protection Systems, Inc., 1993. *Friction Pendulum Seismic Isolation Bearings*, Berkeley, CA.

Hall, J.F., 1999. "Discussion on 'The Role of Damping in Seismic Isolation'," *Earthquake Eng. Struct. Dyn.*, 28, 1717–1720.

Hall, J.F. and K.L. Ryan, 2000. "Isolated Buildings and the 1997 UBC Near-Source Factors," *Earthquake Spectra*, 16, 393–411.

International Code Council (ICC), 2000. *International Building Code*, International Code Council, Falls Church, VA.

Iwan, W.D., 1980. "Estimating Inelastic Response Spectra from Elastic Spectra," *Earthquake Eng. Struct. Dyn.*, 8, 375–388.

Iwan, W.D. and N.C. Gates, 1979. "The Effective Period and Damping of a Class of Hysteretic Structures," *Earthquake Eng. Struct. Dyn.*, 7, 199–221.

Jangid, R.S. and J.M. Kelly, 2000. "Torsional Displacements in Base-Isolated Buildings," *Earthquake Spectra*, 16, 443–454.

Johnson, C.D. and D.A. Kienholz, 1982. "Finite Element Prediction of Damping in Structures with Constrained Viscoelastic Layers," *AIAA J.*, 20, 1284–1290.

Kelly, J. M., 1986. "Aseismic Base Isolation: Review and Bibliography," *Soil Dyn. Earthquake Eng.*, 11, 135–146.

Kelly, J. M., 1993. *Earthquake-Resistant Design with Rubber*, Springer-Verlag, New York.

Kelly, J. M., 1999. "The Role of Damping in Seismic Isolation," *Earthquake Eng. Struct. Dyn.*, 28, 3–20.

Lu, L.Y. and Y.B. Yang, 1997. "Dynamic Response of Equipment in Structures with Sliding Supports," *Earthquake Eng. Struct. Dyn.*, 26, 61–77.

Mayes, R.L. and F. Naiem, 2001. "Design of Structures with Seismic Isolation," in *The Seismic Design Handbook*, 2nd ed., Naiem, F., Ed., Kluwer Academic Publishers, Boston.

Mostaghel, N., M. Hejazi, and J. Tanbakuchi, 1983. "Response of Sliding Structures to Harmonic Support Motions," *Earthquake Eng. Struct. Dyn.*, 11, 355–366.

Naiem, F. and J.M. Kelly, 1999. *Design of Seismic Isolated Structures*, John Wiley & Sons, New York.

Ryan, K.L. and A.K. Chopra, 2002. "Approximate Analysis Methods for Asymmetric Plan Base-Isolated Buildings," *Earthquake Eng. Struct. Dyn.*, 31, 33–54.

Salomon, O., S. Oller, and A. Barbat, 1999. "Finite Element Analysis on Base Isolated Buildings Subjected to Earthquake Loads," *Int. J. Numer. Meth. Eng.*, 46, 1741–1761.

Skinner, R.I., W.H. Robinson, and G.H. McVerry, 1993. *An Introduction to Seismic Isolation*, John Wiley & Sons, New York.

Tsai, C.S., 1997. "Finite Element Formulations for Friction Pendulum Seismic Isolation Bearings," *Int. J. Numer. Meth. Eng.*, 40, 29–39.

Westermo, B. and F. Udwadia, 1983. "Periodic Response of a Sliding Structure to Harmonic Excitation," *Earthquake Eng. Struct. Dyn.*, 11, 135–146.

Yang, Y.B., T.Y. Lee, and I.C. Tsai, 1990. "Response of Multi-Degree-of-Freedom Structures with Sliding Supports," *Earthquake Eng. Struct. Dyn.*, 19, 739–752.

Zayas, V.A., S.S. Low, and S.A. Mahin, 1987. *The FPS Earthquake Resisting System: Experimental Report, Report No. UCB/EERC-87/01, Earthquake Engineering Research Center*, University of California, Berkeley.